Primary rainbow of high refractive index particle (1.547<n<2) has refraction ripples

Yingchun Wu[a], Can Li[a], Cyril Crua[b], Xuecheng Wu[a,d], Sawitree Saengkaew[c], Linghong Chen[a], Gérard Gréhan[c], Kefa Cen[a]

[a] *State Key Laboratory of Clean Energy Utilization, Zhejiang University, Hangzhou, 310027, China*
[b] *Advanced Engineering Centre, University of Brighton, Brighton, BN2 4GJ, UK*
[c] *CNRS UMR 6614/CORIA, BP12, 76801 Saint Etienne du Rouvray, France*
[d] *Corresponding author: wuxch@zju.edu.cn*

Abstract

Primary rainbow (Debye series, p=2) of a common liquid droplet, i.e., water drop, has a smooth Airy rainbow structure, and the superimposed high frequency ripple structures are mostly generated by interference of refraction (p=2) and reflection (p=0). In this work, the primary rainbow (p=2) of a particle with high refractive index ($1.547< n <2$) is found to have ripples. This is because the primary rainbow transits from 2-rays rainbow to 3-rays rainbow. A third refraction light with higher incident angle emerges at the same angle of the classical Airy rainbow, and its interference with the refractions around Descartes ray gives birth to the high frequency ripples. Characteristics of this refraction ripples, i.e., angular frequency, are investigated, and implications of this special ripple for particle measurement are also pointed out. This refraction ripple is not observed in other higher order rainbows.

Keywords: Rainbow, Scattering, Debye series, Ripple, Droplet, Refractive index

1. Introduction

Rainbows, as one of the most fantastic meteorological phenomena, have always drawn attention. The formation of rainbows in nature, i.e., from airborne water droplets, has been extensively studied and understood [1, 2, 3, 4, 5, 6, 7, 8]. The elucidation of the rainbows' mystery have accompanied the development of optics theories, e.g., geometrical optics, wave optics,

electromagnetic optics and quantum optics, and rainbow also serves as a touchstone for them. According to geometrical optics, rainbows of a transparent spherical particle are caused by refraction with one internal reflection at the particle inner surface and appears at the angle of minimum deviation from the direction of incidence. The light intensity of the rainbow is enhanced by the interference of the outgoing waves. The light field of outgoing wave has a cubic wavefront and generates the smooth Airy rainbow structure, which can be modeled by Airy theory and consequently is called Airy rainbow. The Airy rainbow structure is characterized by a main peak which is followed by supernumerary arcs with decreasing intensities. According to the Lorenz-Mie scattering theory, the second order ($p = 2$) of Debye series decomposition of Mie scattering corresponds to it [9, 10], and is called primary rainbow. Its interference with the direct reflection at the outer surface results in ripple structures, which we call reflection ripples in this work, and they together mainly account for the field of light scattering around the primary rainbow angle. In some special cases, other higher orders can have comparable amplitude as the primary rainbow and thus multiple orders of rainbows mix [11], for instance, the primary and fifth orders of rainbow of ethanol ($n = 1.36$). Studies on droplets of the above common liquids with refractive index ranging from 1 to $\sqrt{2}$, conclude that the primary rainbow is smooth and that superimposed ripples are mainly caused by the interference between light scattering of different Debye orders [11].

Moreover, the rainbow phenomenon has been utilized to develop powerful techniques for the experimental diagnostic of droplets and sprays. Since probably the first demonstration of standard rainbow refractometry for droplet refractive index measurement [12], the global rainbow technique [13], one-dimensional rainbow refractometry [14, 15], phase rainbow refractometry [16, 17] and multi-wavelength rainbow imaging [18, 19] have been sequentially proposed. Rainbow refractometry has been applied to characterize a wide range of droplets, including water [20, 21, 22, 23], alkanes [24, 25, 26, 27, 28, 29, 30], kerosene [31], ethanol [32, 14], monoethanolamine [33, 34], diethyl ether [35] and suspensions [36, 37], and flow jets [38, 39] or optical fibers [40] as well. The inversion of rainbow signals for these droplets ($1 < n < \sqrt{2}$) were usually performed based on fast rainbow computation, i.e. Airy theory [41, 42] or Nussenzveig's complex angular momentum (CAM) theory [1, 43, 44], since Lorenz-Mie theory or Debye series is computation consuming. Ouattara et al. [37] studied the rainbow of suspension drops with a low relative refractive index ($n \approx 1.001 - 1.20$) for sizing and mixture

fraction measurement.

However, rainbow behaviors of high refractive index particles have been rarely investigated. In this work, we find that the primary rainbow of a particle with high refractive index ($1.5467< n <2$) has refraction ripples, even *without* interference with the reflected light field. We describe the formation mechanism and present implications for particle measurement techniques in detail below.

2. Analysis

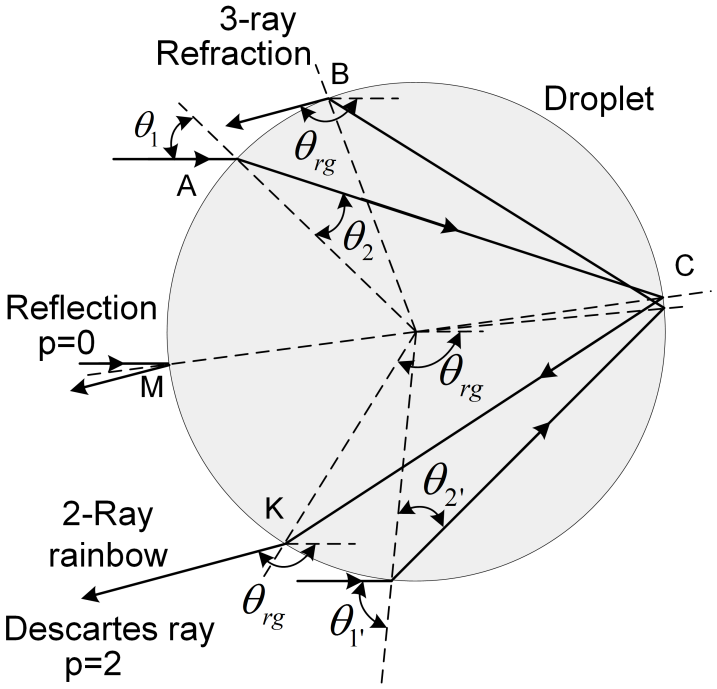

Figure 1: Ray trajectories of the refraction ($p = 2$) and reflection ($p = 0$) light of a particle with high refractive index at the primary rainbow with geometrical optics.

Fig. 1 schematically illustrates the ray trajectories of the light scattering at the primary rainbow angle according to the geometrical optics, the scattering angle (θ) of primary rainbow ($p = 2$) depends on the incident angle (θ_1, $\theta_{1'}$) and refraction angle (θ_2, $\theta_{2'}$), which is determined by Snell's law

$$\theta_2 = \arcsin\left(\frac{\sin\theta_1}{n}\right). \tag{1}$$

The relationship between the incident and scattering angles varies with particle refractive index (n). According to ray trajectory analysis with geometrical optics [1], for a particle of high refractive index with value ranging from $\sqrt{2}$ to 2, there are two possible relationships

$$\theta = \pi - 2\left(2\theta_2 - \theta_1\right), \quad \theta_1 < \theta_{1A}, \tag{2}$$

$$\theta = \pi + 2\left(2\theta_{2'} - \theta_{1'}\right), \quad \theta_{1'} > \theta_{1A}, \tag{3}$$

where the critical incident angle (θ_{1A}) is

$$2\theta_{2A} - \theta_{1A} = 0. \tag{4}$$

Eq. 4 means that the light refracted out of the droplet has 180° angle. Note that Eq. 2 also holds for the classical water rainbow with refractive index $1 < n < \sqrt{2}$.

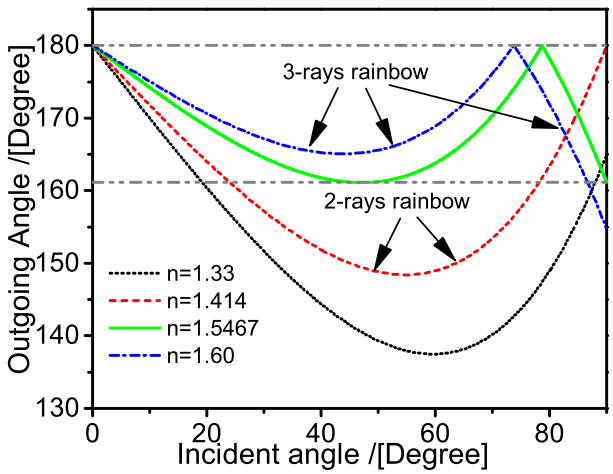

Figure 2: Incident and scattering angles of primary rainbows of particles with different refractive indices.

Fig. 2 shows the scattering angle of Debye ($p = 2$) term with one internal refraction versus incident angle. The scattering angle of a light ray first decreases from 180° to a minimum, and then increases, but remains smaller than 180° when $1 < n < \sqrt{2}$. This minimum deviation angle is a global one and defined as the Airy rainbow position of a particle of this kind.

$$\theta_{rg} = 4\arccos\left(\frac{1}{n}\sqrt{\frac{4-n^2}{3}}\right) - 2\arcsin\left(\sqrt{\frac{n^2-1}{3}}\right). \tag{5}$$

This ray is noted as Descartes ray, with the corresponding incident angle of

$$\cos\left(\theta_{1,rg}\right) = \sqrt{\frac{n^2-1}{3}}. \tag{6}$$

However, as the refractive index increases to $\sqrt{2}$, the scattering angle can reach 180° which is actually a turning point, as shown in Fig. 2. After that, the emerging angle is governed by Eq. 3, and it reverses and decreases with incident angle, down to the rainbow angle at the refractive index ($n_0 = \sqrt{6\sqrt{3}-8} \approx 1.5467$) [1]. However, the deflection angle, which is given by 2, continue increasing. Hence, the definition that the primary rainbow locates at the minimum deflection angle, as governed by Eq. 5, still holds. The rainbow angle is the minimum of the first stationary point of the outgoing angle versus incident angle. It is worth mentioning that the scattering angle continues to decrease and becomes smaller than the former minimum, as evidenced by the curve of $n = 1.60$ in Fig. 2. According to Nussenzveig's notation [1], which was also used by Laven [6], the rainbow can be classified into 2-rays rainbow region for $1 < n < \sqrt{2}$ and 3-rays rainbow region for $1.5467 < n < 2$ using the criterion of the ray number passing rainbow angle, with the intermediate zone being the transition region. While for $n > 2$, there is no turning point, and thus no 2-rays rainbow [1].

3. Results

A representative primary rainbow of a 100 μm particle with refractive index n of 1.55 is calculated with Debye series ($p = 2$) and plotted in Fig. 3(a). Its main peak and first supernumerary resemble these of the classical Airy rainbow of a water drop, as shown in the inset of Fig. 3(a), and decreases in amplitude but increases in frequency with angular position. However, it is surprising that instead of a smooth Airy rainbow structure, ripples superimposed on Airy peaks are observed in Fig. 3(a). The ripples have lower amplitudes and higher frequencies than these of Airy peaks. For a particle with low refractive index, ripples are generated as a result of the interference of external reflection with the smooth Airy rainbow. This explanation is obviously not applicable to this case which has no reflection. As deduced from Fig. 2 and illustrated in Fig. 1, the primary rainbow in Fig. 3 is a 3-ray rainbow. The first two refractions around Descartes ray with small incident angle are governed by Eq. 2, and similar to the 2-ray rainbow of water.

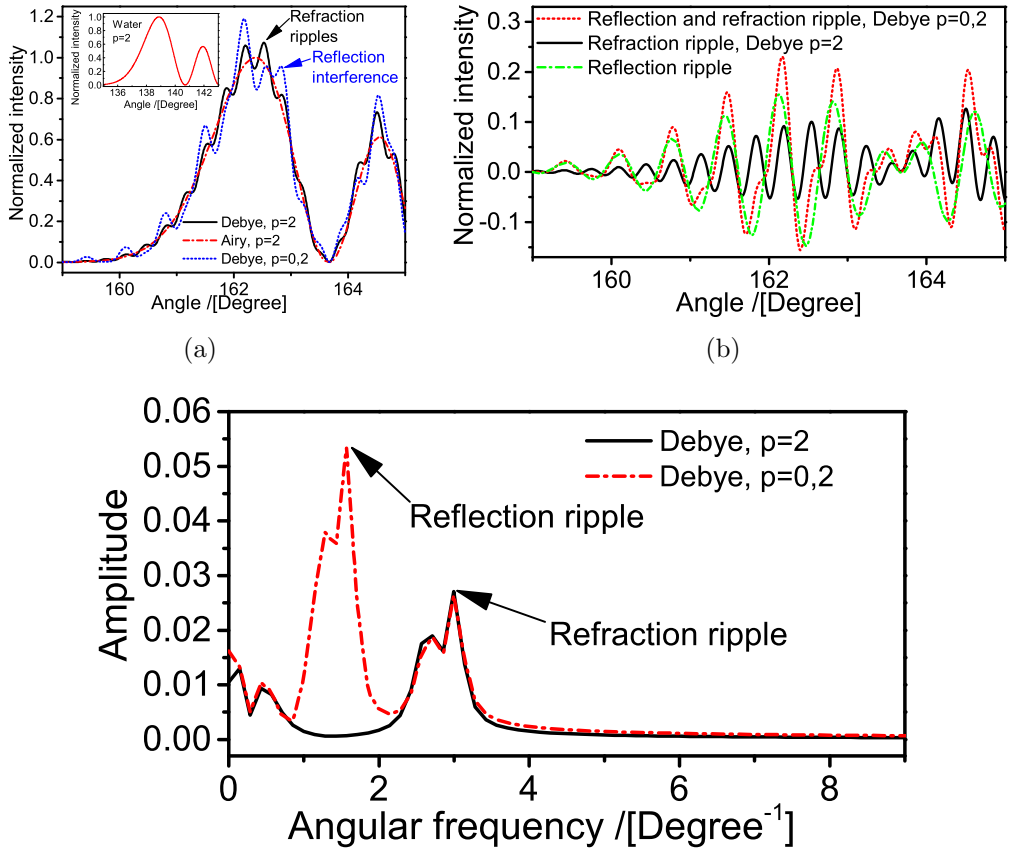

Figure 3: Rainbow light behaviors of a particle with n=1.55 and d=100 μm, under 532 nm laser illumination. (a) Airy rainbow and its comparison with that of Airy theory and Debye series ($p = 0, 2$). (b) Refraction ripples of Airy rainbow and its comparison with reflection ripples. (c) Angular frequencies of rainbow ripples.

Similarly, the light of this part also has a cubic wavefront and generates a smooth rainbow as water, and can be modeled by the Airy theory (please refer to Eq. 21 in [2] for details), as shown in Fig. 3(a). It shows that the smooth rainbow computed by Airy theory penetrates through the ripples on the primary rainbow with Debye series ($p = 2$). The discrepancy between the light scattering computed by Debye series ($p = 2$) and Airy theory, that is, the ripples, suggests that there is another refraction light. As shown in Fig. 1, it is the refraction light that passes through point B, and noted as the

third refraction hereinafter. This coincides with the above analysis of 3-ray rainbow. Analogously, the ripples are interference patterns of this classical smooth Airy rainbow (the first two refractions) with the third refraction light wave, that is parallel to the Descartes ray with a larger incident angle, as illustrated in Fig. 1 and Fig. 2. The scattering angle of the third refraction drops quickly with the incident angle, and therefore the light intensity is much weaker than the former two. Hence, the ripples generated by the interference between the refractions have much lower amplitudes compared with the Airy peaks, and are named refraction ripples thereafter, in order to distinguish from reflection ripples. It is also noticed that the refraction ripples are also observed in the transition region when refractive index is a little smaller than the lower limit ($n_0 = 1.5467$) evaluated from geometrical optics, but its amplitude reduces rapidly to invisible. This is because the outgoing light is a wave and expands to interfere with the former two refractions in the far field.

The light scattering of two Debye orders ($p = 0, 2$), which dominates or even is nearly the same as Mie scattering at the primary rainbow angle since other light scattering processes are negligibly small, is also plotted in Fig. 3(a). A comparison with the primary rainbow ($p = 2$) shows the ripples are modified. This is because the external reflection ($p = 0$) interferes with the smooth Airy rainbow and generates the classical reflection ripples as in the water rainbow, which can be retrieved by subtracting the primary rainbow ($p = 2$) [16], as shown in Fig. 3(b). Similarly, the refraction and the mixed refraction and reflection ripples are respectively yielded by subtracting the Airy rainbow computed with Airy theory from these with orders of ($p = 2$) and ($p = 0, 2$) of Debye series, and are plotted in Fig. 3(b), where the modulation and difference are clearly visualized. The angular spacing of reflection ripples is larger than that of refraction ripples because the reflection glare point M is closer to the Descartes ray point K than the third refraction glare point B, as shown in Fig. 1. Fig. 3(c) is the spectra of primary rainbow ($p = 2$) and standard rainbow ($p = 0, 2$) in Fig. 3(b), and angular frequency peaks corresponding to reflection and refraction ripples are clearly observed. The interference between the external reflection and the outer (third) refraction is negligible since both amplitudes are small. Thus, the high frequency fringes are still dominated by the refraction ripples, although influenced and modulated by the lower frequency reflection ripples.

Similar to interferometric particle imaging (IPI) [45], the angular spacing of the refraction ripple peaks is inversely proportional to the distance of the

two parallel light rays. As shown in Fig. 1, the distance is

$$L_{KB} = 0.5D\left(\sin\theta_1 + \sin\theta_{1'}\right). \tag{7}$$

Analogous to Young's double slit interference, the ripple spacing is

$$\Phi = \frac{2\lambda}{D\left(\sin\theta_1 + \sin\theta_{1'}\right)}. \tag{8}$$

Then the theoretical angular frequency of refraction ripple can be obtained.

Primary rainbows of droplets with refractive indices spanning from 1.55 to 1.70 and diameters ranging from 20 μm to 200 μm are computed with Debye series ($p = 2$), and the refraction ripple frequencies around their rainbow angles are evaluated using Fourier transform, as shown in Fig. 4. The reflection ripple frequency has been intensively studied and thus not duplicated here. We can see that the frequency almost linearly increasing with the droplet size from about 0.5 degree^{-1} at 20 μm to over 5 degree^{-1} at 200 μm, and the linearity indicates that it can be used for size measurement. Note that only several sparse diameters are computed in Fig. 4, while other light phenomena, e.g., morphology dependent resonance (MDR), might dominate the light scattering at some particular droplet diameter if we scan the whole diameter range. For a given droplet size, the refraction ripple frequency slightly decreases (the angular spacing slightly increases) with refractive index, and the variation with respect to the mean (1.625) of the studied refractive indices is within 5%. Although the rainbow angular position strongly depends on droplet refractive index, while the frequencies of refraction ripples exhibit a week dependence on it. A comparison shows that the spacings agree with the theoretical predictions by Eq. 8, collaboratively proving the correctness of the explanation of refraction ripple formation.

High order rainbows, i.e., the secondary ($p = 3$) and third ($p = 4$) rainbows, of the above high refractive index particles are also exploited with Debye series, and they turn out to be smooth and no ripple is observed. A comparison with these computed by Airy theory shows that they agrees well with each other, especially in the first main peak region. This implies that the formation of high order rainbows are the same for both high refractive index particles and ordinary ones, and that they are 2-ray rainbows.

The special feature of Airy rainbow ($p = 2$) of high refractive index ($1.5467 < n < 2$) particles has practical implications for measurements with rainbow refractometry. In the recording, the light from all scattering processes is captured by the sensor, including reflection and refraction ripples, and

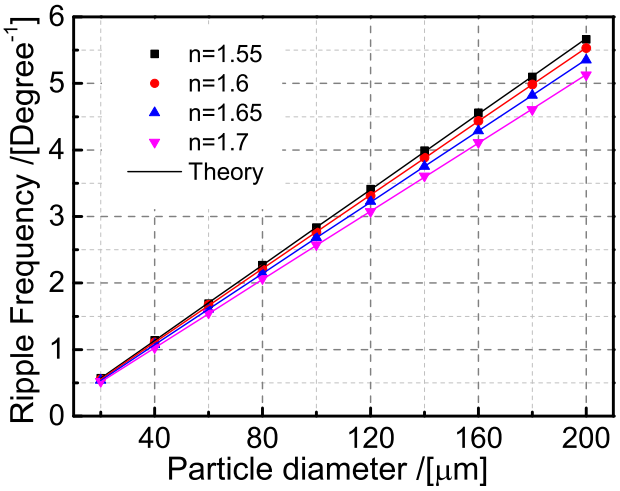

Figure 4: Angular frequencies of refraction ripples of particles with different high refractive indices and sizes.

very limited approaches can be applied to suppress one of them or separate them [18, 46]. Then in the inversion process of standard rainbow refractometry, neither Airy theory nor complex angular momentum theory (Eq. 4.35 in [1]) can accurately inverse the particle refractive index and diameter simultaneously, because theoretically they do not model the refraction ripples in primary rainbow. Thus, Debye series ($p = 0, 2$) and Mie scattering should be used [47], which are computationally intensive. New models are to be developed to achieve high accuracy and fast computation, and one possible approach is to extend the complex angular momentum theory to high refractive index particles. With regard to phase rainbow refractometry for droplet evaporation/condensation measurement [16, 17], the phases of the refraction ripples in primary rainbow and classical reflection ripple structures vary with droplet diameter, and thus two phase shifts will exist. Moreover, the two ripples interfere and overlap, making the phase of the real superimposed ripples present a more complicated behavior. The relationship in [16, 17] only describes the reflection ripples while a new relationship is to be derived for the refraction ripples. As for global rainbow technique, its signal summarizes hundreds and even thousands of polydisperse particles, and smooths both reflection and refraction ripples since both are high frequency, low amplitude and random phase, yielding a smooth Airy rainbow as in previous studies [13, 32]. Thus, the current fast computation algorithm, i.e. Airy and CAM

theories, can be applied for accurate inversion. For particle holography at off-axis primary rainbow angle [48, 49], three systems of holographic rings will be observed, and consequently, three glare points (two refraction and one reflection points) will be reconstructed, as in direct glare point imaging.

4. Conclusions

In conclusion, primary rainbow ($p = 2$) of high refractive index particle ($1.5467 < n < 2$) transits from classical 2-rays rainbow to 3-rays rainbow, and is found to have refraction ripples superimposed on the smooth Airy rainbow structure. This refraction ripples results from the interference between a third refraction with the classical smooth Airy rainbow. The refraction ripple frequency linearly increases with particle diameter and can be used for particle measurement. This extra ripple structures also imply that special attention should be paid to rainbow theory when applying it to inverse particle parameters of this kind.

Acknowledgments: This work was partially supported by the Natural Science Foundation of China (No. 91741129 and 51576177), Innovative Research Groups of the National Natural Science Foundation of China (No. 51621005), Major Program of the National Natural Science Foundation of China (No. 51390491), and the UK's Engineering and Physical Science Research Council [grants EP/K020528/1 and EP/M009424/1].

[1] H. Nussenzveig, Highfrequency scattering by a transparent sphere. ii. theory of the rainbow and the glory, Journal of Mathematical Physics 10 (1969) 125.

[2] R. T. Wang, H. Van de Hulst, Rainbows: Mie computations and the airy approximation, Applied Optics 30 (1) (1991) 106–117.

[3] R. Lee, Mie theory, airy theory, and the natural rainbow, Appl. Opt 37 (1998) 1506–1519.

[4] J. Jackson, From alexander of aphrodisias to young and airy, Physics reports 320 (1) (1999) 27–36.

[5] J. Adam, The mathematical physics of rainbows and glories, Physics reports 356 (4) (2002) 229–365.

[6] P. Laven, Effects of refractive index on glories, Applied Optics 47 (34) (2008) H133–H142. doi:10.1364/AO.47.00H133.
URL http://ao.osa.org/abstract.cfm?URI=ao-47-34-H133

[7] P. Laven, Rainbows, Coronas and Glories, Springer, 2012, pp. 193–222.

[8] A. Haumann, Rainbows in nature: recent advances in observation and theory, European Journal of Physics 37 (6) (2016) 063001.

[9] H. C. Hulst, H. Van De Hulst, Light scattering by small particles, Courier Corporation, 1957.

[10] P. Laven, Simulation of rainbows, coronas and glories using mie theory and the debye series, Journal of Quantitative Spectroscopy and Radiative Transfer 89 (1) (2004) 257–269. doi:https://doi.org/10.1016/j.jqsrt.2004.05.026.
URL http://www.sciencedirect.com/science/article/pii/S0022407304001840

[11] R. Li, X. Han, H. Jiang, K. F. Ren, Debye series for light scattering by a multilayered sphere, Appl. Opt. 45 (6) (2006) 1260–1270.
URL http://ao.osa.org/abstract.cfm?URI=ao-45-6-1260

[12] N. Roth, K. Anders, A. Frohn, Refractive-index measurements for the correction of particle sizing methods, Appl. Opt. 30 (33) (1991) 4960–4965.
URL http://ao.osa.org/abstract.cfm?URI=ao-30-33-4960

[13] J. Van Beeck, D. Giannoulis, L. Zimmer, M. Riethmuller, Global rainbow thermometry for droplet-temperature measurement, Optics letters 24 (23) (1999) 1696–1698.

[14] X. Wu, H. Jiang, Y. Wu, J. Song, G. Gréhan, S. Saengkaew, L. Chen, X. Gao, K. Cen, One-dimensional rainbow thermometry system by using slit apertures, Optics Letters 39 (3) (2014) 638–641. doi:10.1364/OL.39.000638.
URL http://ol.osa.org/abstract.cfm?URI=ol-39-3-638

[15] Y. Wu, J. Promvongsa, X. Wu, K. Cen, G. Grehan, S. Saengkaew, One-dimensional rainbow technique using fourier domain filtering, Optics Express 23 (23) (2015) 30545–30556. doi:10.1364/OE.23.030545.

URL http://www.opticsexpress.org/abstract.cfm?URI=oe-23-23-30545

[16] Y. Wu, J. Promvongsa, S. Saengkaew, X. Wu, J. Chen, G. Gréhan, Phase rainbow refractometry for accurate droplet variation characterization, Optics Letters 41 (20) (2016) 4672–4675. doi:10.1364/OL.41.004672.
URL http://ol.osa.org/abstract.cfm?URI=ol-41-20-4672

[17] Y. Wu, C. Crua, H. Li, S. Saengkaew, L. Mädler, X. Wu, G. Gréhan, Simultaneous measurement of monocomponent droplet temperature/refractive index, size and evaporation rate with phase rainbow refractometry, Journal of Quantitative Spectroscopy and Radiative Transfer 214 (2018) 146–157. doi:https://doi.org/10.1016/j.jqsrt.2018.04.034.
URL https://www.sciencedirect.com/science/article/pii/S0022407318300748

[18] W. Schäfer, C. Tropea, W. Elsäßer, Determination of size and refractive index of a single water droplet by using a light source with short coherence length (led), in: 15th International Symposium on Applications of Laser Techniques to Fluid Mechanics, Lisbon, Schäfer, Walter Tropea, Cameron Elsäer, Wolfgang.

[19] X. Wu, H. Jiang, K. Cao, Y. Wu, C. Li, G. Gréhan, S. Saengkaew, K. Cen, Self-calibrated global rainbow refractometry: a dual-wavelength approach, Chinese Optics Letters 15 (4) (2017) 042902.
URL http://col.osa.org/abstract.cfm?URI=col-15-4-042902

[20] J. van Beeck, L. Zimmer, M. Riethmuller, Global rainbow thermometry for mean temperature and size measurement of spray droplets, Particle & Particle Systems Characterization 18 (4) (2001) 196–204.

[21] P. Lemaitre, E. Porcheron, G. Grehan, L. Bouilloux, Development of a global rainbow refractometry technique to measure the temperature of spray droplets in a large containment vessel, Measurement Science and Technology 17 (2006) 1299.

[22] M. Vetrano, S. Gauthier, J. van Beeck, P. Boulet, J. Buchlin, Characterization of a non-isothermal water spray by global rainbow thermometry, Experiments in Fluids 40 (1) (2006) 15–22.

[23] H. Yu, F. Xu, C. Tropea, Spheroidal droplet measurements based on generalized rainbow patterns, Journal of Quantitative Spectroscopy and Radiative Transfer 126 (2013) 105–112.

[24] P. Massoli, F. Beretta, A. D'Alessio, M. Lazzaro, Temperature and size of single transparent droplets by light scattering in the forward and rainbow regions, Applied Optics 32 (18) (1993) 3295–3301.

[25] J. Wilms, B. Weigand, Composition measurements of binary mixture droplets by rainbow refractometry, Applied Optics 46 (11) (2007) 2109–2118.

[26] C. Letty, B. Renou, J. Reveillon, S. Saengkaew, G. Gréhan, Experimental study of droplet temperature in a two-phase heptane/air v-flame, Combustion and Flame.

[27] C. D. Rosebrock, S. Shirinzadeh, M. Soeken, N. Riefler, T. Wriedt, R. Drechsler, L. Mädler, Time-resolved detection of diffusion limited temperature gradients inside single isolated burning droplets using rainbow refractometry, Combustion and Flame 168 (2016) 255–269.

[28] H. Li, C. D. Rosebrock, T. Wriedt, L. Mädler, The effect of initial diameter on rainbow positions and temperature distributions of burning single-component n-alkane droplets, Journal of Quantitative Spectroscopy and Radiative Transfer 195 (2017) 164–175. doi:https://doi.org/10.1016/j.jqsrt.2017.01.004.
URL http://www.sciencedirect.com/science/article/pii/S002240731630591X

[29] J. Promvongsa, P. Vallikul, B. Fungtammasan, A. Garo, G. Grehan, S. Saengkaew, Multicomponent fuel droplet evaporation using 1d global rainbow technique, Proceedings of the Combustion Institute 36 (2) (2017) 2401–2408. doi:http://dx.doi.org/10.1016/j.proci.2016.08.010.
URL http://www.sciencedirect.com/science/article/pii/S1540748916303996

[30] A. Verdier, J. Marrero Santiago, A. Vandel, S. Saengkaew, G. Cabot, G. Grehan, B. Renou, Experimental study of local flame structures and fuel droplet properties of a spray jet flame, Proceedings of the Combustion Institute 36 (2) (2017) 2595–2602.

doi:https://doi.org/10.1016/j.proci.2016.07.016.
URL http://www.sciencedirect.com/science/article/pii/S1540748916302723

[31] S. Sankar, D. Buermann, W. Bachalo, Application of rainbow thermometry to the study of fuel droplet heat-up and evaporation characteristics, Journal of engineering for gas turbines and power 119 (1997) 573.

[32] X. Wu, Y. Wu, S. Saengkaew, S. Meunier-Guttin-Cluzel, G. Gréhan, L. Chen, K. Cen, Concentration and composition measurement of sprays with a global rainbow technique, Measurement Science and Technology 23 (12) (2012) 125302.

[33] M. Ouboukhlik, S. Saengkaew, M.-C. Fournier Salan, L. Estel, G. Grehan, Local measurement of mass transfer in a reactive spray for co2 capture, The Canadian Journal of Chemical Engineering 93 (2) (2015) 419–426.

[34] M. Ouboukhlik, G. Godard, S. Saengkaew, M.-C. Fournier-Salan, L. Estel, G. Grehan, Mass transfer evolution in a reactive spray during carbon dioxide capture, Chemical Engineering & Technology 38 (7) (2015) 1154–1164. doi:10.1002/ceat.201400651.
URL http://dx.doi.org/10.1002/ceat.201400651

[35] J. L. Marie, N. Grosjean, L. Mees, M. Seifi, C. Fournier, B. Barbier, M. Lance, Lagrangian measurements of the fast evaporation of falling diethyl ether droplets using in-line digital holography and a high-speed camera, Experiments in Fluids 55 (4). doi:10.1007/s00348-014-1708-6.

[36] M. Vetrano, J. Petrus Antonius Johannes van Beeck, M. Riethmuller, Global rainbow thermometry: improvements in the data inversion algorithm and validation technique in liquid-liquid suspension, Applied Optics 43 (18) (2004) 3600–3607.

[37] M. Ouattara, F. Lamadie, M. P. L. Sentis, F. R. A. Onofri, Droplet sizing and mixture fraction measurement in liquid-liquid flows with rainbow-angle diffractometry, Applied Optics 56 (29) (2017) 8109–8120. doi:10.1364/AO.56.008109.
URL http://ao.osa.org/abstract.cfm?URI=ao-56-29-8109

[38] X. Han, K. F. Ren, Z. Wu, F. Corbin, G. Gouesbet, G. Gréhan, Characterization of initial disturbances in a liquid jet by rainbow sizing, Applied optics 37 (36) (1998) 8498–8503.

[39] F. Song, C. Xu, S. Wang, Rainbow technique for multi-parameter measurement of absorbing cylinder, Particuology 11 (2) (2013) 184–188.

[40] G. wirniak, J. Mroczka, Approximate solution for optical measurements of the diameter and refractive index of a small and transparent fiber, JOSA A 33 (4) (2016) 667–676.

[41] J. Johannes van Beeck, T. Grosges, M. De Giorgi, Global rainbow thermometry assessed by airy and lorenz-mie theories and compared with phase doppler anemometry, Applied Optics 42 (19) (2003) 4016–4022.

[42] M. Vetrano, J. Antonius Johannes van Beeck, M. Riethmuller, Generalization of the rainbow airy theory to nonuniform spheres, Optics Letters 30 (6) (2005) 658–660.

[43] S. Saengkaew, T. Charinpanitkul, H. Vanisri, W. Tanthapanichakoon, L. Mees, G. Gouesbet, G. Grehan, Rainbow refractrometry: on the validity domain of airys and nussenzveigs theories, Optics communications 259 (1) (2006) 7–13.

[44] S. Saengkaew, T. Charinpanikul, C. Laurent, Y. Biscos, G. Lavergne, G. Gouesbet, G. Grehan, Processing of individual rainbow signals, Experiments in Fluids 48 (1) (2010) 111–119.

[45] S. Dehaeck, J. van Beeck, Designing a maximum precision interferometric particle imaging set-up, Experiments in Fluids 42 (5) (2007) 767–781. doi:10.1007/s00348-007-0286-2.
URL http://dx.doi.org/10.1007/s00348-007-0286-2http://download.springer.com/static/pdf/861/art%253A10.1007%252Fs00348-007-0286-2.pdf?originUrl=http%3A%2F%2Flink.springer.com%2Farticle%2F10.1007%2Fs00348-007-0286-2&token2=exp=1486483499~acl=%2Fstatic%2Fpdf%2F861%2Fart%25253A10.1007%25252Fs00348-007-0286-2.pdf%3ForiginUrl%3Dhttp%253A%252F%252Flink.springer.com%252Farticle%252F10.1007%252Fs00348-007-0286-2*~hmac=c10e9acdadac6021b413560fbfd1d90529c33046523bea5cd4074ffe7280f25e

[46] W. Schäfer, C. Tropea, Time-shift technique for simultaneous measurement of size, velocity, and relative refractive index of transparent droplets or particles in a flow, Applied Optics 53 (4) (2014) 588–597. doi:10.1364/AO.53.000588.
URL http://ao.osa.org/abstract.cfm?URI=ao-53-4-588http://www.opticsinfobase.org/DirectPDFAccess/76251C69-B80C-18B2-9267857C01BBD07E_277764/ao-53-4-588.pdf?da=1&id=277764&seq=0&mobile=no

[47] F. Song, C. Xu, S. Wang, Y. Yan, An optimization scheme for the measurement of liquid jet parameters with rainbow refractometry based on debye theory, Optics Communications 305 (0) (2013) 204–211. doi:http://dx.doi.org/10.1016/j.optcom.2013.04.027.
URL http://www.sciencedirect.com/science/article/pii/S0030401813003957http://ac.els-cdn.com/S0030401813003957/1-s2.0-S0030401813003957-main.pdf?_tid=6d177aa2-6cc0-11e4-83bb-00000aacb35f&acdnat=1416053624_0bd05c18d7cf69cb32216c58e82d98f9

[48] Y. Wu, X. Wu, S. Saengkaew, S. Meunier-Guttin-Cluzel, L. Chen, K. Qiu, X. Gao, G. Gréhan, K. Cen, Digital gabor and off-axis particle holography by shaped beams: A numerical investigation with glmt, Optics communications 305 (0) (2013) 247–254. doi:http://dx.doi.org/10.1016/j.optcom.2013.05.009.
URL http://www.sciencedirect.com/science/article/pii/S0030401813004847

[49] Y. Wu, X. Wu, L. Yao, M. Brunel, S. Coëtmellec, R. Li, D. Lebrun, H. Zhou, G. Gréhan, K. Cen, Characterizations of transparent particle holography in near-field using debye series, Applied Optics 55 (3) (2016) A60–A70.
URL http://ao.osa.org/abstract.cfm?URI=ao-55-3-A60